Fbxw7 is a driver of uterine carcinosarcoma by promoting epithelial-mesenchymal transition

Ileana C. Cuevas[a], Subhransu S. Sahoo[a], Ashwani Kumar[b], He Zhang[c], Jill Westcott[d], Mitzi Aguilar[a], Jeremy D. Cortez[a], Stephanie A. Sullivan[e], Chao Xing[b], D. Neil Hayes[f], Rolf A. Brekken[d,g,h], Victoria L. Bae-Jump[i], and Diego H. Castrillon[a,g,j,1]

[a]Department of Pathology, The University of Texas Southwestern Medical Center, Dallas, TX 75390; [b]Eugene McDermott Center for Human Growth and Development, The University of Texas Southwestern Medical Center, Dallas, TX 75390; [c]Quantitative Biomedical Research Center, Department of Population and Data Sciences, The University of Texas Southwestern Medical Center, Dallas, TX 75390; [d]Hamon Center for Therapeutic Oncology Research, The University of Texas Southwestern Medical Center, Dallas, TX 75390; [e]Gynecologic Oncology, Massey Cancer Center, Virginia Commonwealth University, Richmond, VA 23298; [f]Division of Medical Oncology and Center for Cancer Research, University of Tennessee Health Science Center, Memphis, TN 38163; [g]Simmons Comprehensive Cancer Center, The University of Texas Southwestern Medical Center, Dallas, TX 75390; [h]Department of Pharmacology, The University of Texas Southwestern Medical Center, Dallas, TX 75390; [i]Division of Gynecologic Oncology, Lineberger Comprehensive Cancer Center, University of North Carolina, Chapel Hill, NC 27599; and [j]Department of Obstetrics and Gynecology, The University of Texas Southwestern Medical Center, Dallas, TX 75390

Edited by Guillermina Lozano, University of Texas MD Anderson Cancer Center, Houston, TX, and approved October 31, 2019 (received for review July 3, 2019)

Uterine carcinosarcoma is an aggressive variant of endometrial carcinoma characterized by unusual histologic features including discrete malignant epithelial and mesenchymal components (carcinoma and sarcoma). Recent studies have confirmed a monoclonal origin, and comprehensive genomic characterizations have identified mutations such as *Tp53* and *Pten*. However, the biological origins and specific combination of driver events underpinning uterine carcinosarcoma have remained mysterious. Here, we explored the role of the tumor suppressor *Fbxw7* in endometrial cancer through defined genetic model systems. Inactivation of *Fbxw7* and *Pten* resulted in the formation of precancerous lesions (endometrioid intraepithelial neoplasia) and well-differentiated endometrioid adenocarcinomas. Surprisingly, all adenocarcinomas eventually developed into definitive uterine carcinosarcomas with carcinomatous and sarcomatous elements including heterologous differentiation, yielding a faithful genetically engineered model of this cancer type. Genomic analysis showed that most tumors spontaneously acquired *Trp53* mutations, pointing to a triad of pathways (p53, PI3K, and Fbxw7) as the critical combination underpinning uterine carcinosarcoma, and to Fbxw7 as a key driver of this enigmatic endometrial cancer type. Lineage tracing provided formal genetic proof that the uterine carcinosarcoma cell of origin is an endometrial epithelial cell that subsequently undergoes a prominent epithelial–mesenchymal transition underlying the attainment of a highly invasive phenotype specifically driven by Fbxw7.

uterine carcinosarcoma | Pten | Fbxw7 | epithelial-mesenchymal transition | Tp53

Endometrial carcinoma (EC), which arises in the endometrial lining of the uterine corpus, is a common malignancy in women, with over 60,000 cases anticipated in the United States this year (1). Most cases are well-differentiated and of the endometrioid subtype, where all of the malignant cells are epithelial and form glands resembling those of normal endometrium. Such cancers are usually confined to the uterus at the time of diagnosis, and, for such tumors, the prognosis is good. However, the other principal EC histologic subtypes—serous carcinoma, clear cell carcinoma, and carcinosarcoma—are of higher histologic grade and have a much worse prognosis (2). Among these, uterine carcinosarcoma (UCS; previously known as malignant mixed Müllerian tumor [MMMT]) is by far the most lethal, with a tendency for early and widespread metastases and an estimated 5-y survival of only 30%. UCS accounts for only 3% of endometrial cancers, but 16% of deaths (3).

UCS is an intriguing EC subtype defined by "biphasic" histology consisting of admixed malignant epithelial and mesenchymal (i.e., carcinomatous and sarcomatous) components (2). The epithelial component is low or high grade and resembles either endometrioid or serous adenocarcinoma (4). The mesenchymal component can be "homologous" with types of differentiation native to the uterus, such as smooth muscle or endometrial stroma. Remarkably, however, the mesenchymal component is conspicuously "heterologous" in half of cases, exhibiting, for example, obvious cartilaginous or osseous differentiation (chondrosarcoma or osteosarcoma) (5).

Historically, UCS was considered a sarcoma, but recent studies have argued it represents a variant of uterine carcinoma. For example, UCS shares epidemiologic features and patterns of chromosomal instability with high-grade carcinomas, and also shares mutational spectra with ECs, including frequent mutations in loci encoding PI3K pathway components (6–8). Comparison of

Significance

Uterine carcinosarcoma (UCS) is an aggressive endometrial cancer variant distinguished from endometrial adenocarcinoma (EC) by admixed malignant epithelial and mesenchymal components (carcinoma and sarcoma). The molecular events underlying UCS are enigmatic, as cancer gene mutations are generally shared among UCS/EC. We take advantage of genetic approaches in mice to show that inactivation of *Fbxw7* and *Pten* results in UCS through spontaneous acquisition of mutations in a third gene (*Tp53*), arguing for strong biological selection and synergism in UCS. We used this UCS model including tumor-derived cell lines to show that Fbxw7 loss drives epithelial–mesenchymal transition, explaining Fbxw7's role in UCS. This model system argues that simultaneous genetic defects in 3 distinct pathways (Fbxw7, Pten/PI3K, Tp53) converge in UCS genesis.

Author contributions: I.C.C. and D.H.C. designed research; I.C.C., S.S.S., J.W., and D.H.C. performed research; I.C.C., M.A., J.D.C., S.A.S., D.N.H., R.A.B., V.L.B.-J., and D.H.C. contributed new reagents/analytic tools; I.C.C., A.K., H.Z., C.X., and D.H.C. analyzed data; and I.C.C. and D.H.C. wrote the paper.

The authors declare no competing interest.

This article is a PNAS Direct Submission.

Data deposition: RNA sequence data reported in this paper have been deposited in the Gene Expression Omnibus (GEO) database, https://www.ncbi.nlm.nih.gov/geo (accession no. GSE138490). DNA sequence data reported in this paper have been deposited in the National Center for Biotechnology Information (NCBI) Sequence Read Archive, https://www.ncbi.nlm.nih.gov/bioproject (accession no. PRJNA543538).

[1]To whom correspondence may be addressed. Email: diego.castrillon@utsouthwestern.edu.

This article contains supporting information online at https://www.pnas.org/lookup/suppl/doi:10.1073/pnas.1911310116/-/DCSupplemental.

First published November 26, 2019.

microdissected epithelial and mesenchymal components from individual patients has revealed common chromosomal alterations and mutations, arguing for a monoclonal origin (9–11). Systematic genomic characterizations of UCS have identified frequent mutations in some genes, most notably *Tp53*, but such mutations also frequently occur in serous and high-grade endometrioid cancers and are not specific to UCS (6). These findings, taken together, thus beg the question as to the nature of the specific molecular driver(s) of EMT/sarcomatous differentiation in UCS. Also, whether the UCS cell of origin is epithelial or mesenchymal (and whether the presence of the 2 components represents an epithelial–mesenchymal transition or conversely a mesenchymal–epithelial transition) cannot be definitively ascertained from human studies. No definitive precursor lesion has been described for UCS, adding further uncertainty as to its histogenesis.

Fbxw7 (previously known as CDC4) is a tumor suppressor that functions as the substrate recognition component of an E3 SCF-type ubiquitin ligase complex controlling the degradation of key cell growth regulators including c-Myc, Cyclin E, Notch1, Klf5, and mTOR (12–14). Fbxw7 targets are regulated in a tissue-specific and/or developmental manner (15, 16). *Fbxw7* mutations characterize diverse cancers (hematopoietic, colon, stomach, gallbladder/bile duct). In women, carcinomas of the lower female reproductive tract (the Müllerian system), including the uterine cervix and corpus, frequently harbor *Fbxw7* mutations. Indeed, uterine cancers have the highest incidence of *Fbxw7* mutations among all human cancers, followed by colon cancer (17). Although many *Fbxw7* mutations are heterozygous and include missense mutations in the substrate binding or WD40 domain and are believed to act in a dominant-negative manner, a significant number of mutations are truncating or otherwise loss-of-function. This spectrum of *Fbxw7* mutations appears to have similar biochemical consequences, resulting in the inactivation of Fbxw7 and stabilization of Fbxw7 cell type-specific substrates. Concordantly, in diverse nongynecologic mouse models, both the WD40 and truncating mutations have proven potently oncogenic (14, 18–20).

Notwithstanding the importance of *Fbxw7* in EC as evidenced by its high mutation rate (10 to 20%) (17, 21), little is known about its biological functions as an endometrial tumor suppressor. Despite numerous studies of Fbxw7 in other cancer types in mice, no Fbxw7-based mouse models of EC have been generated to date. In this study, we engineered an endometrial-specific Cre driver and used it to investigate the role of *Fbxw7* as an endometrial tumor suppressor through concerted genetic analyses in mice, complemented with investigations of human uterine cancer samples. These investigations revealed an unexpected role of Fbxw7 as a driver of EMT in the genesis of UCS.

Results

***BAC-Sprr2f-Cre*, an Improved Endometrial Cre Driver for Genetically Engineered EC Models.** We previously showed that the murine *Sprr2f* gene is expressed only in the uterus, and therein only within endometrial epithelium, the presumptive cell of origin for all ECs. In these prior studies, a 5.5-kb *Sprr2f* promoter fragment was fused to *Cre* to generate a "minigene" transgenic driver line *Sprr2f-Cre*, a.k.a. *Tg(Sprr2f-cre)*^{1Dcas} (22). This allele drives Cre-mediated recombination in endometrial epithelium and has been used in the generation of EC models (23–25). However, one limitation is ectopic Cre expression, including in kidney and cerebellum. Since the endogenous *Sprr2f* gene is expressed only in the uterus and not in these other tissues, we surmised that undesired ectopic activity was due to the small promoter fragment and absence of distant regulatory elements repressing nonendometrial expression (22).

To overcome these limitations, we took advantage of bacterial artificial chromosome (BAC) RP23-39I4 (26), which harbors a 189-kb C57/B6 genomic fragment spanning the *Sprr2* tandem gene cluster on chromosome 3. Recombineering methods were used to replace the *Sprr2f* coding sequence with a *Cre* ORF at the ATG start codon in exon 2 (Fig. 1*A*). The *Neo* selection cassette was then excised by transient flippase expression, and the resulting engineered BAC was injected into mouse oocytes for generation of a transgenic *BAC-Sprr2f-Cre* founder line. In BAC transgenesis, integration occurs at random chromosomal locations. The site of integration for *BAC-Sprr2f-Cre* was not determined, but is autosomal based on its Mendelian pattern of inheritance.

Crosses to the *Rosa26* β-galactosidase reporter (*R26R*) (27) were conducted to compare patterns of Cre-mediated recombination of the original *Sprr2f-Cre* versus the *BAC-Sprr2f-Cre* line. No Cre activity was observed with *R26R* alone, as expected. With the original *Sprr2f-Cre* allele, extensive Cre-mediated recombination was observed in the uterus (endometrial epithelium), kidney (tubular epithelium), and cerebellum (Purkinje cells), as previously reported. In contrast, with the new BAC allele, ectopic expression in cerebellum and kidney was abolished, while recombination efficiency in endometrium was unaltered (Fig. 1*B*). Ectopic expression in fallopian tube epithelium was also abolished (Fig. 1*C*). In *BAC-Sprr2f-Cre;R26R* uteri, endometrial epithelium exhibited ∼50% recombination by 6 wk of age. This recombination efficiency (i.e., subtotal, mosaic) is useful for genetically engineered mouse models of EC, as it recapitulates the admixture of genetically normal and abnormal epithelial cells that characterize the initial stages of endometrial carcinogenesis (28). Cre-mediated recombination was not observed in sexually immature *BAC-Sprr2f-Cre;R26R* mice at 3 wk of age, but was efficiently induced by β-estradiol (Fig. 1*D*). This confirms that the estrogen dependence of the *Sprr2f* locus (which harbors estrogen response elements) is retained with *BAC-Sprr2f-Cre* and also that Cre-mediated recombination can be induced early by β-estradiol administration (22).

***Fbxw7* and *Pten* Potently Synergize to Drive ECs in Mice.** *Fbxw7* mutations in human EC were first reported in 2002 (29), but their significance and high incidence (∼20% of cases) was not fully appreciated until genome sequencing efforts confirmed and extended the initial results (21). Despite the crucial contribution of *Fbxw7* mutation in EC, few studies have focused on the biological basis of its function as an endometrial tumor suppressor in vivo. To develop an animal model to explore these critical questions, we first studied *Fbxw7* inactivation alone. *BAC-Sprr2f-Cre* was bred to mice harboring a floxed *Fbxw7*^{L} allele, where *LoxP* sites flank essential exons 5 to 6 (14). The absence of tumors up to 1 y of age in *BAC-Sprr2f-Cre*;*Fbxw7*$^{L/L}$ females (abbreviated *Fbxw7*) implied that *Fbxw7* inactivation alone was insufficient to drive ECs (Fig. 2*A*) and that other cooperating genetic events contribute. This is also consistent with observations that ECs with *Fbxw7* mutations harbor multiple oncogenic mutations. Several observations pointed to *Pten* inactivation as a potential cooperating genetic event. First, the PI3K pathway is frequently dysregulated in EC, and *Pten*, a potent inhibitor of PI3K signaling, is the most frequently mutated gene in EC (30). Analyzing the Uterine Corpus EC TCGA data through cBioPortal (31), we found that, of 43 *Fbxw7* mutant cases, all but 8 had mutations in canonical PI3K pathway genes. Furthermore, *Pten* was the PI3K pathway gene mutated in the highest percentage of cases (25/43, 58%), followed by *Pik3ca* (20/43, 47%).

To investigate cooperation between *Fbxw7* and *Pten* in endometrial carcinogenesis, cohorts of double mutant *BAC-Sprr2f-Cre*;*Fbxw7*$^{L/L}$;*Pten*$^{L/L}$ (abbreviated *Fbxw7*/*Pten*) were established for longitudinal studies including survival analysis. Cohorts of single gene knockout *Fbxw7* or *Pten* mice were also generated. In contrast to *Fbxw7*-alone mice, *Fbxw7*/*Pten* mice developed uterine cancers starting at 12 wk of age. The tumors were bulky but localized, typically involving only 1 of the 2 uterine horns (Fig. 2*B*). Clonal losses of Pten protein were confirmed immunohistochemically. By 6 wk, Pten was lost in ∼50% of epithelial cells, and these clones also showed increased p-Akt(Ser473), consistent

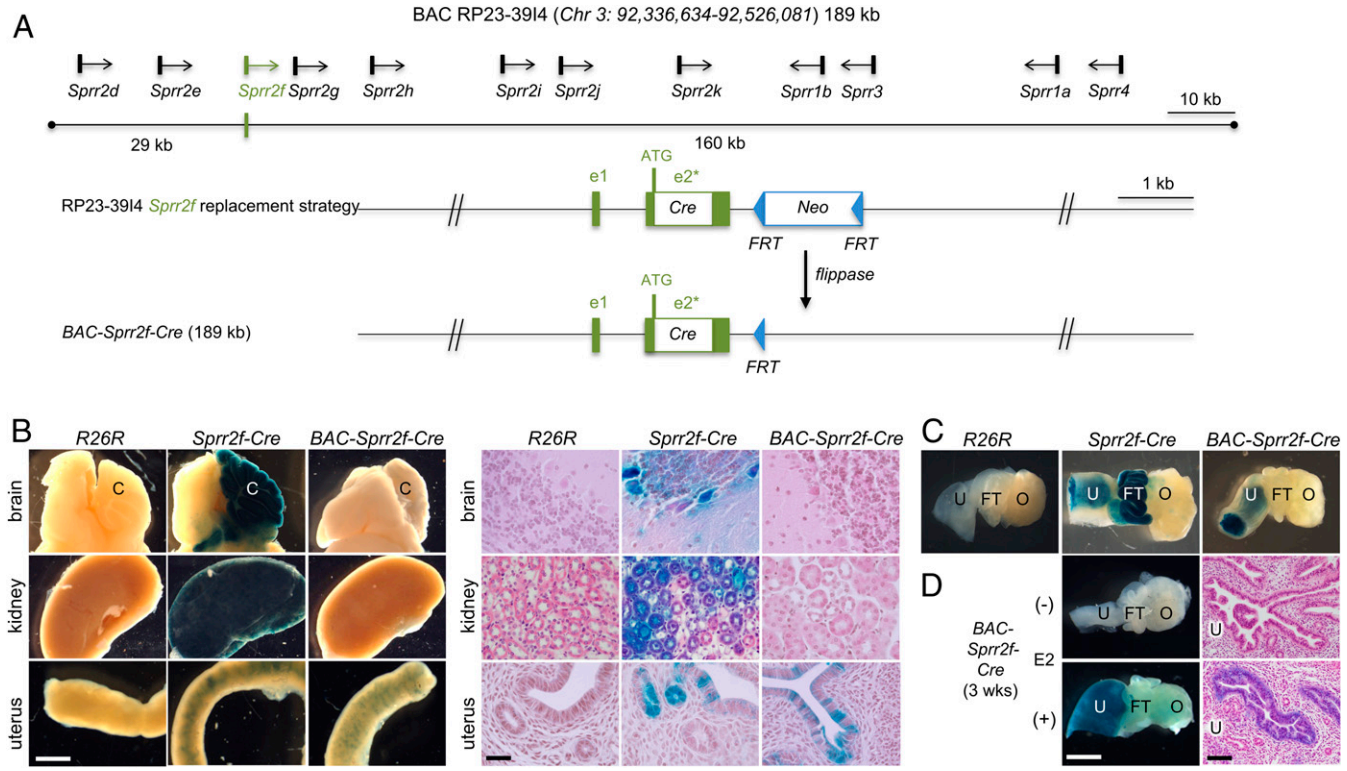

Fig. 1. Generation of an endometrial-specific Cre driver. (*A*) BAC targeting strategy to generate *BAC-Sprr2f-Cre* construct and transgenic mice. Direction of transcription is shown for all *Sprr2* genes in BAC RP23-39I4 189 kb genomic fragment based on end-sequencing of insert. The *Sprr2f* ORF is entirely encoded within exon 2. *FRT*, sites for flippase recombination. (*B*) Evaluation of Cre-mediated recombination in mice harboring *R26R* β-galactosidase reporter only, *Sprr2f-Cre;R26R*, and *BAC-Sprr2f-Cre;R26R*. Tissues were stained with X-gal: gross (*Left*) and histological (*Right*) analysis of slides counterstained with H&E. C, cerebellum. (Scale bars: gross photographs, 2 mm; photomicrographs, 20 μm.) (*C*) Analysis of Müllerian structures including uterus ("U"), fallopian tube (FT), and ovary ("O"). With *BAC-Sprr2f-Cre*, ectopic expression in FT was eliminated. (*D*) Impact of treatment with 17β-estradiol (E2) at 3 wk of age. E2 diffusely induced recombination in endometrial epithelial cells. Sections counterstained with H&E. (Scale bars: gross photographs, 2 mm; photomicrographs, 45 μm.)

with Akt hyperactivation. This led to complete relocalization of the transcription factor and Akt target Foxo1 from the nucleus to the cytoplasm, as occurs in human endometrial precancers and other PI3K-dependent developmental and reproductive processes (32–34). By 12 wk, *Fbxw7/Pten* uteri showed an increased percentage of *Pten*-null cells relative to *Pten* alone ($P = 0.027$, t test), showing that *Fbxw7* and *Pten* loss act synergistically in conferring a growth advantage to endometrial epithelial cells (*SI Appendix*, Fig. S1 *A* and *B*).

Uterine weights and histology confirmed striking cooperativity between the 2 tumor suppressors. *Fbxw7* mice exhibited only small increases in uterine weight, and, while *Pten* mice showed larger increases, this was due to florid endometrial hyperplasia (a.k.a. endometrioid intraepithelial neoplasia [EIN]) without invasion (Fig. 2*C*). By 24 wk of age, the difference in uterine weights between *Fbxw7/Pten* vs. control mice was statistically significant ($P < 0.0025$, t test), and this difference became even more significant at 36 wk of age ($P < 0.0001$, t test). Furthermore, 75% of *Fbxw7/Pten* mice exhibited myometrial invasion by 24 wk, vs. 0% for *Pten*. Survival analysis confirmed the striking synergism, with a median survival of 352 d for *Fbxw7/Pten* vs. 568 d for *Pten* and 603 d for *Fbxw7* (Fig. 2*D*). Per log-rank analysis, survival of *Fbxw7/Pten* mice was significantly decreased vs. *Fbxw7*, *Pten*, or control mice ($P < 0.0001$ for each of the pairwise comparisons). *Fbxw7* mice showed slightly but significantly increased survival vs. *Pten* alone ($P = 0.0151$; Fig. 2*D*).

***Fbxw7/Pten* Uterine Invasive Cancers Are Initially Endometrioid Adenocarcinomas that Unexpectedly Progress to Carcinosarcoma.** To investigate histologic progression and behavior of cancers in this model, *Fbxw7/Pten* mice were necropsied at 6, 12, 24, and 36 wk ($n = 6$ to 10 per time point; Fig. 3). By only 6 wk of age, 90% of mice exhibited striking endometrioid intraepithelial neoplasia (EIN), the histologic precursor for endometrioid adenocarcinoma (2). EIN lesions were characterized by hypercellularity, glandular complexity, and absence of invasion, closely mimicking human EIN (Fig. 3*B*). While it is difficult to reliably identify invasion within endometrium (i.e., into endometrial stroma) in humans or mice, the presence of malignant glands/epithelium in myometrium is a definite indicator of invasion in mouse models of EC (22, 35, 36). By 12 wk, 55% of uteri exhibited myometrial invasion, with some exhibiting full-thickness invasion (Fig. 3*B*). All invasive cancers at 12 wk of age were adenocarcinomas with endometrioid histology and were of an entirely epithelial character. Notably, 50% of these cancers exhibited $p63^+$ squamous differentiation by 24 wk of age, a distinctive hallmark of human EC seen in ≥25% of cases (Fig. 3*B*) (37). By 36 wk, 80% of the mice harbored invasive ECs.

Histological analyses at 40 to 67 wk revealed a striking, systematic, and unexpected shift of overall tumor histotype. By 67 wk ($n = 30$), all cancers became biphasic, with distinct but admixed epithelial (carcinomatous) and mesenchymal (sarcomatous) components. The epithelial components consisted of endometrioid adenocarcinoma sometimes with admixed squamous carcinoma. The mesenchymal components consisted of high-grade spindle cells with high mitotic index and high-grade nuclear atypia (undifferentiated sarcoma). Even more strikingly, 100% of these tumors also contained malignant heterologous elements with cartilaginous or osseous differentiation, i.e., chondrosarcoma or osteosarcoma.

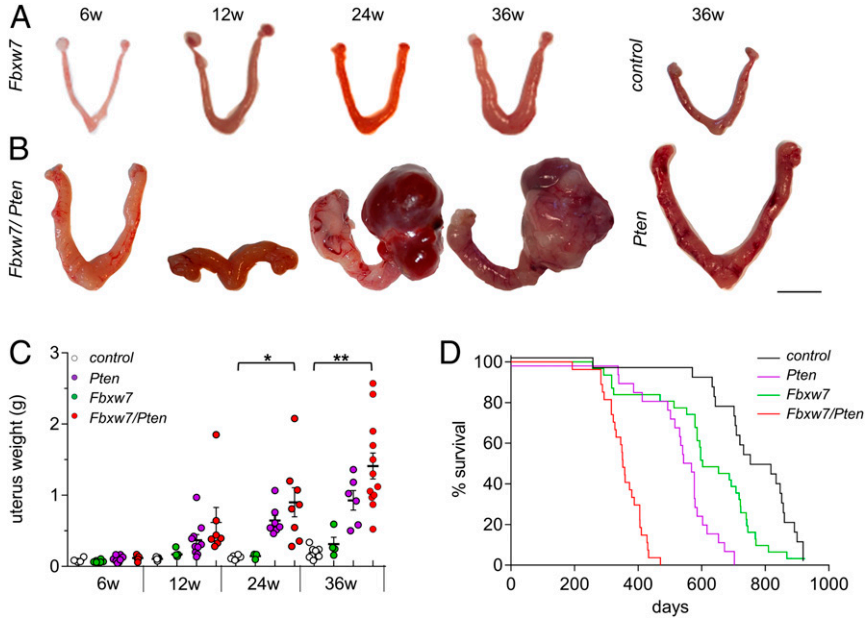

Fig. 2. Potent synergism between *Fbxw7* and *Pten* tumor suppressors in endometrial carcinogenesis. (*A*) Gross photographs of *BAC-Sprr2f-Cre;Fbxw7*$^{L/L}$ (*Fbxw7*) uteri at 6 to 36 wk. (*Right*) Littermate control uterus from 36-wk-old *Fbxw7*$^{L/L}$;*Pten*$^{L/L}$ (*Cre* negative) mouse. (*B*) Gross photographs of *BAC-Sprr2f-Cre;Fbxw7*$^{L/L}$;*Pten*$^{L/L}$ (*Fbxw7*/*Pten*) uteri at 6 to 36 wk. (*Right*) Littermate control uterus from 36-wk-old *Pten* mouse. For *A* and *B*, uterine silhouettes were digitally cropped from dark background to more clearly show uterine morphology. (*C*) Uterine weights; $n \geq 6$ mice per time point (*$P < 0.0025$; **$P < 0.0001$, *t* test). (*D*) Kaplan–Meier survival analysis. Standard tumor burden criteria (not death) per IACUC guidelines were used (*Materials and Methods*). Cohorts were *Fbxw7*$^{L/L}$;*Pten*$^{L/L}$ (*Cre* negative, $n = 21$), *BAC-Sprr2f-Cre;Pten*$^{L/L}$ ($n = 23$), *BAC-Sprr2f-Cre;Fbxw7*$^{L/L}$ ($n = 30$), and *BAC-Sprr2f-Cre;Fbxw7*$^{L/L}$;*Pten*$^{L/L}$ ($n = 27$). The *Fbxw7*/*Pten* vs. control, *Fbxw7*/*Pten* vs. *Pten,* and *Fbxw7*/*Pten* vs. *Fbxw7* curves are statistically different ($P < 0.0001$, log-rank test).

We then performed lineage tracing in this UCS model with the *mTmG* reporter (38) that, upon Cre-mediated recombination, switches from membrane Tomato (red) to membrane green fluorescent protein expression, providing a lineage marker stably inherited over subsequent cell divisions. In *mTmG;BAC-Sprr2f-Cre* females, Cre activity was observed only in endometrial epithelium, with no recombination in endometrial stroma (only endometrial glands turned green). In older females harboring UCS ($n = 3$), the sarcomatous and carcinomatous components expressed only green fluorescent protein. This lineage tracing provides formal proof that UCS, including any sarcomatous elements, is ultimately derived from the endometrial epithelium (*SI Appendix*, Fig. S2 *A* and *B*).

Concordant with the aggressive behavior of human UCS, most mice harbored distant metastases to ≥1 site, and these were carcinomatous, sarcomatous, or both. All *Fbxw7*/*Pten* mice in the survival analysis had metastasis to adjacent organs (ovary, peritoneum), while 58% (15/26) showed distant metastasis. The organs with highest frequency of metastasis were liver (53%), lung (40%), colon (27%), kidney (20%), and spleen (13%), and 4/15 mice showed metastasis to ≥1 organ. We conclude that *Fbxw7*/*Pten* tumors begin as usual-type endometrioid adenocarcinomas, but evolve in a surprisingly stereotypical manner between 12 and 48 wk into definitive UCS. This is remarkable, as UCS has not been reported among prior mouse models of EC, many of which were based on *Pten* or *Trp53* (35, 39–41). These findings thus point to *Fbxw7* as a specific driver of UCS. *Fbxw7*/*Pten* mice represent a faithful mouse model of human UCS, with 100% penetrance for this histotype. Also, since Cre was expressed solely in the epithelial compartment, the model, together with the *mTmG* lineage tracing, provides formal genetic proof that the UCS cell of origin is an endometrial epithelial cell that subsequently undergoes EMT.

Unbiased Analyses Reveal that *Trp53* Is the Critical Third Cooperating Oncogene in *Fbxw7/Pten*-Driven Murine UCS. The focality of cancers in *Fbxw7*/*Pten* uteri (Fig. 2*B*) strongly suggested that additional, presumably stochastic genetic event(s) drove tumor formation. DNA from 7 formalin-fixed, paraffin-embedded (FFPE) tumors from mice at 28 to 61 wk of age and paired normal samples such as liver were subjected to gene resequencing using a custom hybrid capture panel of 76 murine genes, including all loci corresponding to those frequently mutated in human ECs of all histotypes (*SI Appendix*, Table S1). DNA obtained from normal tissue served as a matched germline control for reliable identification of somatically acquired mutations (Fig. 4*A*) (42).

Of the 76 genes, only one—*Trp53*, the murine homolog of human *TP53*—was mutated in ≥1 tumor (Fig. 4*B*). All 4 of these tumors harbored mutations leading to amino acid substitutions (A135V, H165R, V170M, R172H) previously documented as recurring cancer drivers in human tumors (43). For example, murine R172H corresponds to the human R175H dominant-negative hotspot mutation, and an engineered R172H allele also functions as a genetically dominant oncogene in mice (44–46), while murine A135V corresponds to the temperature-sensitive A138V *TP53* mutation (47). Only one other mutation was identified among the 76 loci in the 7 cases: *Kras*^{G12D} in a tumor with no *Trp53* mutation but with a "mutant pattern" of p53 overexpression (as detailed later and in Fig. 4*B*).

p53 mutations lead to abnormal accumulation of the protein, making immunohistochemistry (IHC) an extremely reliable surrogate for mutations (48). Whereas control endometria did not express p53 by IHC, 6 of the 7 tumors subjected to sequencing displayed marked overexpression of p53, including 3 of 4 tumors without mutations by sequence analysis (Fig. 4 *B* and *C*). These results demonstrate that p53 is inactivated in a substantial majority of *Fbxw7*/*Pten* ECs. Intragenic or larger deletions spanning *TP53*/*Trp53* are common cancer-driving events not detectable by exon resequencing, and may account for the observed overexpression/presumptive mutation of p53 protein in the UCS not harboring *Trp53* missense mutations (48).

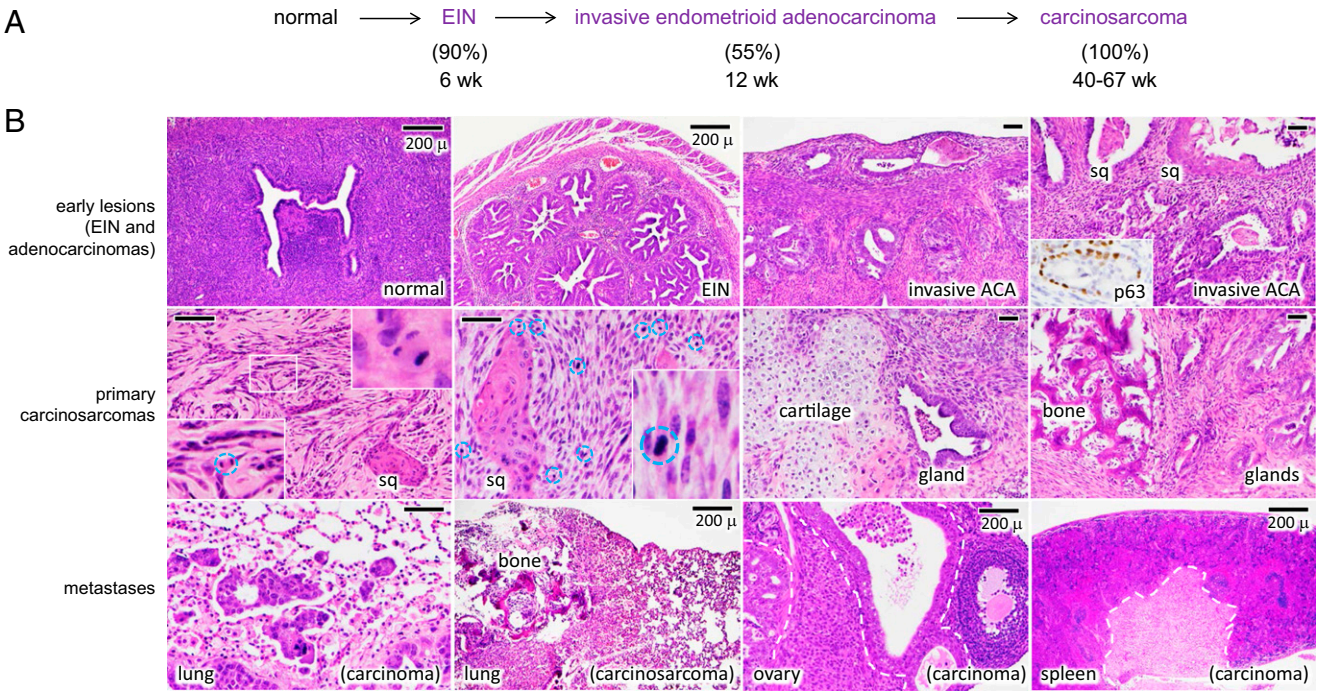

Fig. 3. Cancer initiation and progression to UCS in *Fbxw7*/*Pten* mice. (*A*) Summary of progression per histologic analyses. (*B*, *Top*) Normal endometrium at 12 wk and early noninvasive endometrioid intraepithelial neoplasia (EIN) with preneoplastic architectural features (cell and gland crowding) starting at 6 wk. EIN lesions develop into invasive endometrioid adenocarcinomas (ACA) starting at 12 wk with definitive invasion of malignant glands into myometrium. Some cases exhibit squamous differentiation (sq) confirmed by p63 immunostaining (*Inset*). (*B*, *Middle*) UCS with overtly malignant mesenchymal and epithelial components. The epithelial components are glandular or squamous (sq), whereas mesenchymal components consist of malignant spindle cells with frequent and aberrant mitotic figures (small dashed circles and insets) and foci of malignant cartilage (chondrosarcoma) or bone (osteosarcoma). (*B*, *Bottom*) Metastases to peritoneum and peritoneal organs such as ovary and more distant metastasis. Metastatic foci were carcinomatous or carcinosarcomatous. Metastatic deposits highlighted in some panels with dashed white lines. (Scale bars: 50 μm, except where noted.)

To expand upon these results, p53 IHC was performed on a larger set of *Fbxw7*/*Pten* tumors. We killed randomly selected mice at 12, 24, and 36 wk (n = 8, 8, and 11, respectively), and also analyzed 27 mice that were subjected to necropsy as part of formal survival analysis (at 39 to 67 wk). Consistent with the aforementioned results, p53 overexpression was not detected in mouse uteri at 12 wk in tumorous or normal endometrium. However, the incidence of p53 clonal overexpression by IHC increased over time, reaching 80% in mice euthanized due to illness per tumor burden criteria (Fig. 4 *D* and *E*). Of note, some human tumors (those with truncating mutations) exhibit complete loss of p53 expression (so-called null pattern) (48), but this pattern would not be readily detectable due to low levels of p53 protein expression in normal mouse uterine cells, hampering the ability to reliably detect p53 loss relative to adjacent normal cells. Thus, the incidence of p53 inactivation in these tumors may be >80%. Three of the 4 cases (75%) harboring *Tp53* mutations exhibited metastases, vs. 4 of 6 (67%) with either *Tp53* mutation or mutant-pattern expression p53 and 22 of 27 (78%) among all mice analyzed as part of the survival curve. These differences are not statistically significant.

Interestingly, p53 overexpression was detected in many cases by the invasive adenocarcinoma stage (before appearance of sarcoma). For example, at 24 wk, when no tumors exhibited overt UCS features, 40% of tumors already harbored distinctive p53-mutant clones (Fig. 4*E*). In UCS in older animals, p53 overexpression was observed in both epithelial and mesenchymal components. p53 overexpression (and, by inference, mutation) did not exhibit 1:1 correlation with areas of UCS, either temporally or spatially. These results are similar to human UCS, which typically shows aberrant p53 expression but often only in focal areas, demonstrating that *TP53* mutation is a late event (4). Thus, while combined *Fbxw7*/*Pten*/*Trp53* inactivation appear to be obligate synergistic events in the evolution of UCS, the combination leads to cellular differentiation events not manifest immediately in *Trp53*-null clones. These findings also suggest that the precursor lesion for UCS can be a preexisting endometrioid adenocarcinoma harboring this mutational triad.

Expression Profiling Reveals a Critical Role for Fbxw7 in Mediating EMT in Uterine Cancers. Cell lines were established from *Fbxw7*/*Pten* UCS at 49 and 56 wk of age (UCS1 and UCS2). To devise an inducible system to study Fbxw7's biological functions in UCS, a wild-type *Fbxw7* cDNA was cloned into a doxycycline-inducible "tet-on" lentiviral construct (pLVX-Fbxw7). Induction with doxycycline resulted in only a modest increase of Fbxw7 protein by Western analysis. We surmised that the modest induction of protein was due to mRNA features such as suboptimal codon utilization limiting protein translation, and synthesized an *Fbxw7* cDNA sequence optimized for expression in mammalian cells. The codon-optimized cDNA was cloned into the same lentiviral vector, and the resulting construct (pLVX-Fbxw7opt) resulted in higher Fbxw7 protein levels (*SI Appendix*, Fig. S3*A*). UCS1 and UCS2 were transduced with pLVX-Fbxw7opt and subjected to drug selection. Following addition of doxycycline, efficient and concentration-dependent induction of Fbxw7 was documented for both cell lines. As expected, Akt was hyperphosphorylated in UCS1 and UCS2 due to the deficiency of Pten, and induction of Fbxw7 did not have a major impact on Akt phosphorylation levels (*SI Appendix*, Fig. S3 *B* and *C*).

Fbxw7 induction destabilized several canonical Fbxw7 target proteins, including c-Myc, Notch-1 intracellular domain (NICD Val1744), and Krüppel-like factor 5 (Klf5; Fig. 5*A*), demonstrating that these known Fbxw7 targets likely mediate the actions of Fbxw7 mutations in uterine cancer (14, 20, 49–51). To gain

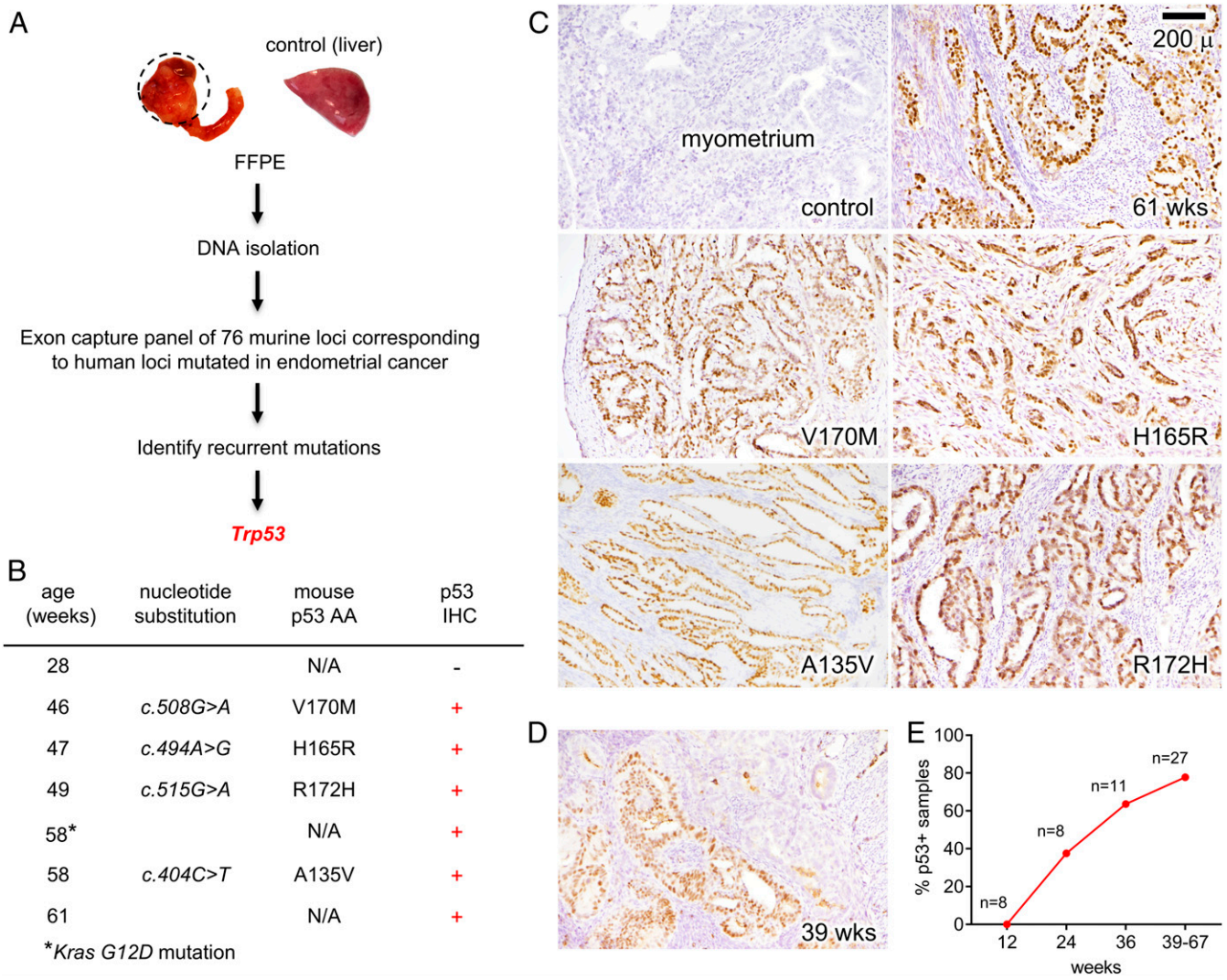

B

age (weeks)	nucleotide substitution	mouse p53 AA	p53 IHC
28		N/A	-
46	*c.508G>A*	V170M	+
47	*c.494A>G*	H165R	+
49	*c.515G>A*	R172H	+
58*		N/A	+
58	*c.404C>T*	A135V	+
61		N/A	+

Fig. 4. Unbiased sequencing analyses identify *Trp53* mutation as critical cooperating genetic event in genesis of UCS. (*A*) Genomic DNA was isolated from FFPE from tumor and control tumor-free tissue (usually liver) from same mouse and hybridized to a custom capture panel of 76 murine loci corresponding to human loci frequently mutated in EC. *Trp53* was the only gene mutated in >1 sample. (*B*) Table summarizing next generation sequencing (NGS) results and p53 immunostaining. Only one other mutation ($Kras^{G12D}$) was identified among the tumors. (*C*) Representative p53 IHC on normal (control) uterus showing lack of p53 expression, all 4 tumors harboring *Trp53* mutations, and 1 of the tumors not harboring a *Trp53* mutation (labeled 61 wk). (*D*) Example of p53 IHC in expanded set of *Fbxw7*/*Pten* tumors not subjected to NGS. This tumor was an endometrioid adenocarcinoma (that had not yet evolved into a UCS). In this field, the presence of $p53^+$ malignant glands next to p53 wild-type glands reveals that p53 became inactivated in an endometrioid adenocarcinoma component (i.e., prior to morphologically recognizable UCS). (*E*) Presence of $p53^+$ positive foci in *Fbxw7*/*Pten* uteri. p53 IHC was performed at 12, 24, and 36 to 67 wk of age. The *y* axis indicates percentage of animals with $p53^+$ foci.

broader insights into Fbxw7's functions, UCS1 and UCS2 cells were again infected with pLVX-Fbxw7 lentivirus (+/−), treated with doxycycline, and subjected to transcriptomic profiling by RNA-seq of 3 separately induced biological replicates generated by splitting into 3 separate cell cultures (12 samples total) (52). Fbxw7 induction exerted a dramatic and reproducible impact on the transcriptome. Using stringent criteria (FDR <0.001, log cpm >0), expression levels of 295 and 59 genes were altered in UCS1 and UCS2, respectively (Fig. 5*B*). Of note, the UCS1/2 gene sets showed significant overlap (48 genes; *P* value = $1.5e^{-78}$; *Materials and Methods*). Heat map profiling of the overlapping genes at FDR <0.001 confirmed that gene-expression alterations were uniform among biological replicates in UCS1/2 (Fig. 5*C*). Gene Ontology analyses for the larger UCS1 gene set revealed significant enrichment for cell adhesion, cell migration, extracellular matrix organization, Notch signaling, cell matrix adhesion, and positive regulation of EMT, among other GO terms (Fig. 5*D* and *SI Appendix*, Table S2 *A–C*). Similar results were obtained for UCS2 (*SI Appendix*, Fig. S4 and Table S2 *D–F*). The differentially expressed genes include drivers of EMT such as Notch1, Hey ligand, Met, Tgfβ1, Pdgfrα/β, and extracellular matrix factors believed to be downstream participants in EMT, such as Mmp2, Adamts14, and multiple genes encoding collagen and osteoid/chondroid matrix factors. The differentially expressed GO categories, genes within each GO category, and differentially expressed genes are tabulated for UCS1/2 in *SI Appendix*, Table S2 *A–F*. Overall, these results point to Fbxw7 as a potent cell-reprogramming factor and specific driver of EMT in UCS.

To validate these studies, selected differentially expressed genes were subjected to Western or RT-PCR analysis. Pdgfrß and collagen 15α1 protein levels were lower following Fbxw7 induction, concordant with RNA-seq (Fig. 5*E*). In addition, several other EMT regulators, including Zeb-1, Twist, β-catenin, and Snail were also down-regulated following Fbxw7 reexpression (Fig. 5*E*).

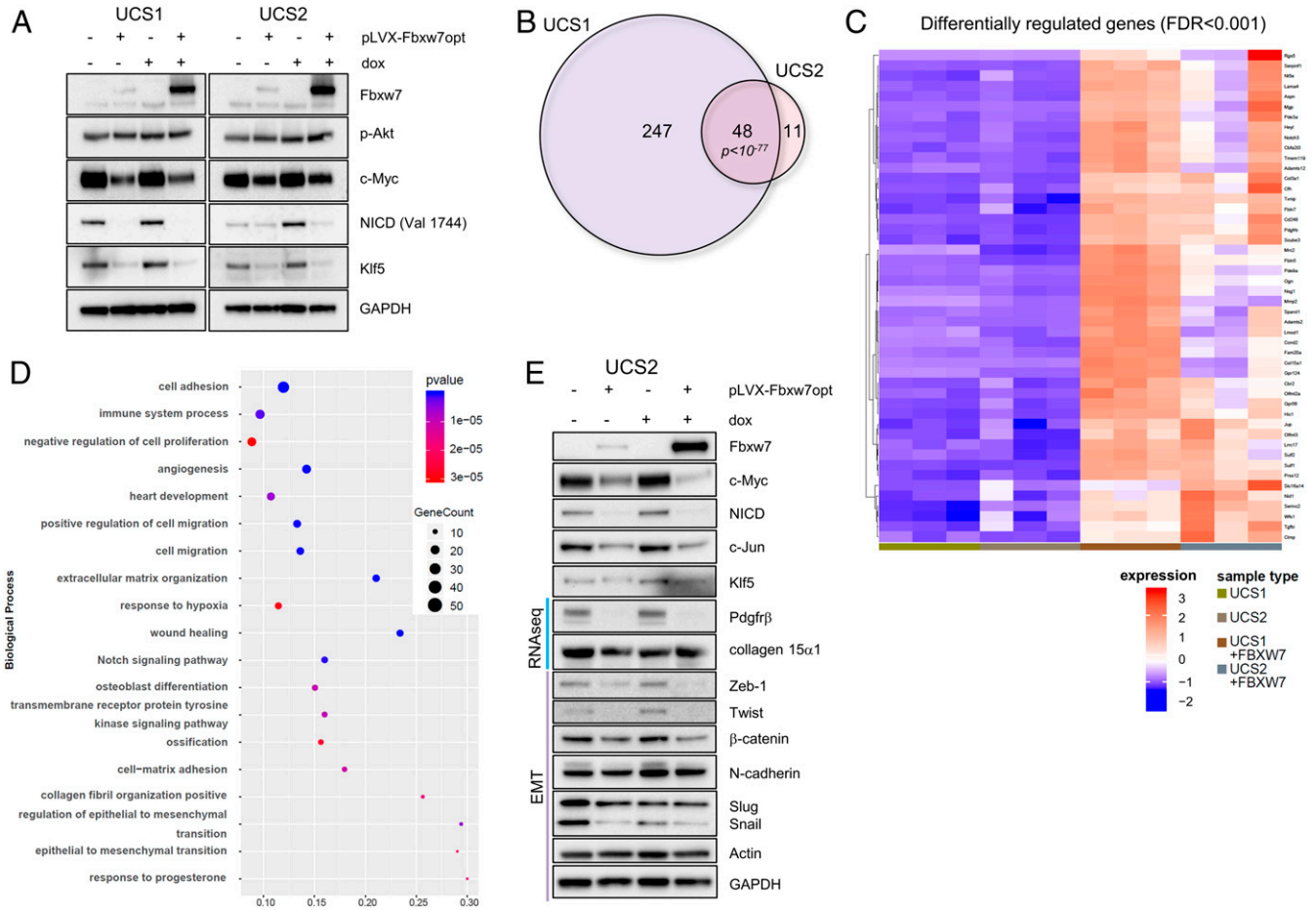

Fig. 5. Fbxw7 is master regulator of EMT in UCS. (*A*) Western blot analysis of UCS1 and UCS2 after transfection with empty vector (–) or with pLVX-Fbxw7opt (+). UCS1 and UCS2 were grown +/– 500 ng/mL doxycycline (dox) for 18 h. (*B*) Venn diagram of differentially expressed transcripts in UCS1 and UCS2 following Fbxw7 reexpression. (*C*) Heat map showing expression patterns of 48 differentially expressed genes across UCS1/2. The log change expression of the transcripts between UCS1/2 +/– Fbxw7 is denoted as red (up-regulated) or blue (down-regulated). (*D*) Dot plot representation of significant GO categories for UCS1 (DAVID). (*E*) Western blot analysis of additional factors examined in UCS2.

However, some EMT-related proteins such as N-cadherin or Slug were not appreciably altered (Fig. 5*E*). Leaky expression of the codon-optimized Fbxw7 prior to induction was sufficient to at least partially destabilize targets, with further decreases in protein levels following induction (e.g., c-Myc). We also confirmed differential RNA expression of other genes including *HeyL* (Notch signaling), *Fibulin 5/7* (cell adhesion and extracellular matrix organization), *Olfml2a* (extracellular matrix organization), *Mmp2* (angiogenesis, positive regulation of cell migration), and *Mgp* (ossification; *SI Appendix*, Fig. S5).

Evidence for Functional Synergism between PI3K Pathway and Fbxw7 via Gsk3β. Efficient binding of Fbxw7 to target proteins (and hence their degradation) depends on phosphorylation of the degron motif by Gsk3β, creating a phospho-degron. Gsk3β in turn is directly regulated by Akt. Akt phosphorylates Gsk3β, which results in decreased Gsk3β activity and decreased phosphorylation of target degrons (13, 17, 53). To document such potential interactions in this UCS model, we analyzed Gsk3β in the UCS1/2 cell lines. Gsk3β was highly expressed in both lines, and total Gsk3β levels were slightly lower following Fbxw7 reexpression (*SI Appendix*, Fig. S6*A*). Treatment with the PI3K inhibitor LY294002 greatly inhibited Gsk3β(Ser9) phosphorylation, confirming that Gsk3β is constitutively phosphorylated by Akt in UCS1/2. This result argues that observed genetic synergism between Fbxw7 and PI3K/Pten pathways is likely to be mediated at least in part by Gsk3β. Concordantly, c-Myc levels were reduced by Fbxw7 reexpression, and this was further enhanced by PI3K inhibition. In cell growth assays with UCS1/2, Fbxw7 reexpression or PI3K inhibition caused decreased cell growth, but both together exerted a potent synergistic effect (*SI Appendix*, Fig. S6*B*). In conclusion, these results argue that the Fbxw7 and PI3K/Pten pathways synergize in UCS through Gsk3β through effects on the stability of Fbxw7 targets such as c-Myc, as previously shown in diverse contexts (13, 17, 53).

Functional Studies Implicate Fbxw7 in Cell Migration and Invasion in Uterine Carcinosarcoma. We then studied the role of Fbxw7 in cellular phenotypes related to cancer initiation and progression. Reexpression of Fbxw7 in UCS1/2 showed a consistent, albeit modest, impact on cell proliferation (Fig. 6*A*), consistent with prior studies showing that Fbxw7 loss promotes cell proliferation through c-Myc and Cyclin E (17). This was also consistent with the growth advantage of *Fbxw7/Pten* vs. *Pten* cells documented in vivo (*SI Appendix*, Fig. S1*B*). Fbxw7 reexpression impacted cell motility and wound closure in a 2D cell culture system (Fig. 6*B*) as well as chemotaxis and migration through Matrigel in a Transwell migration assay (Fig. 6*C*). Moreover, in a separate organotypic experimental culture system, Fbxw7 restricted the ability of cells to extend "invasive" cellular protrusions into the extracellular matrix (Fig. 6*D*). We then enforced expression of the degradation-resistant mutant c-MycT58A. Gsk3β phosphorylates c-Myc at T58,

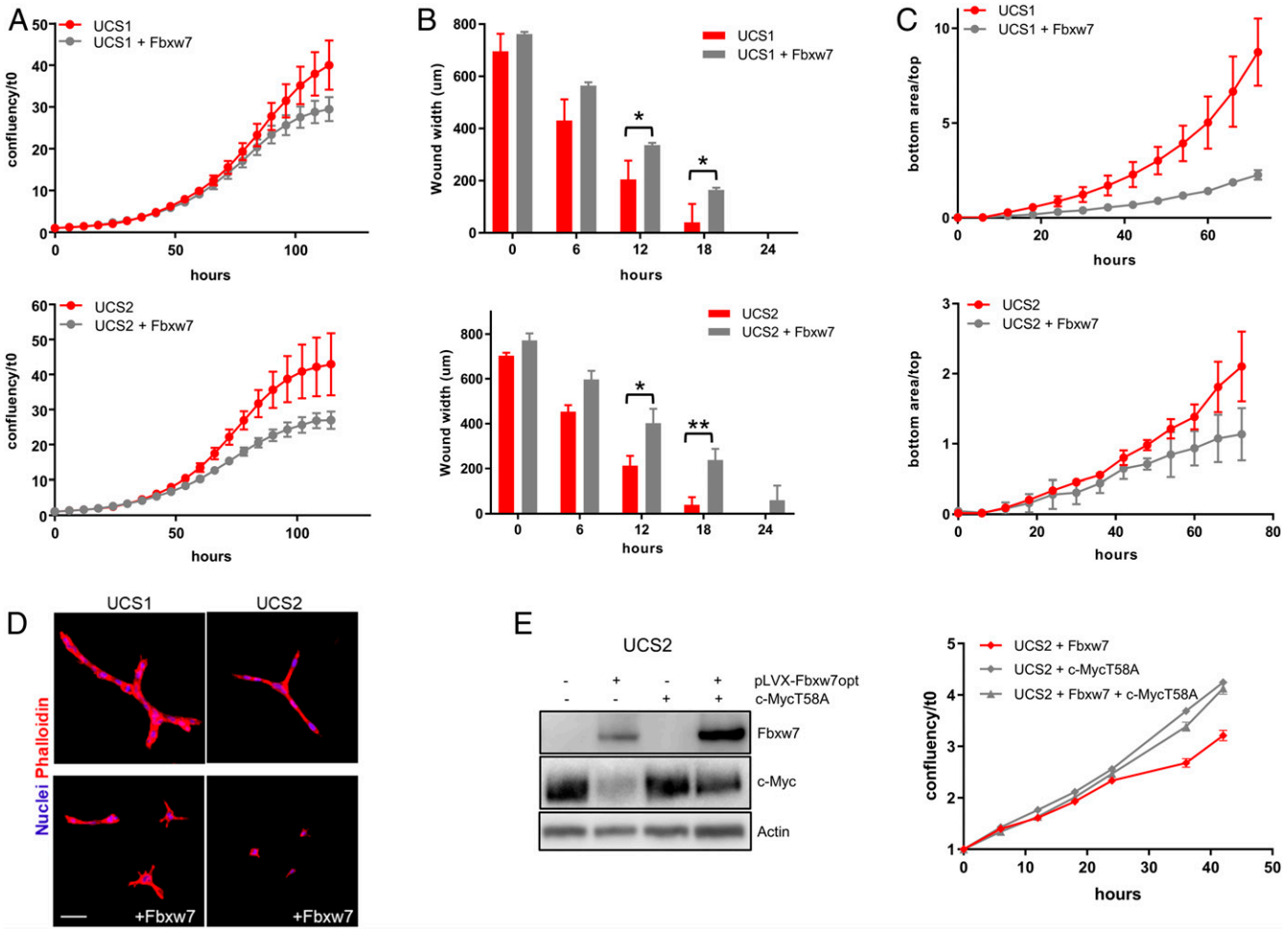

Fig. 6. Fbxw7 inhibits migration and invasion of UCS cells. (*A*) Proliferation expressed as ratio of confluency relative to time 0 (t0). (*B*) Cell migration assays following scratch wound (*$P < 0.05$; **$P < 0.005$, *t* test). (*C*) Cell migration per chemotaxis. Cells were seeded over matrigel in FBS 0.5% and allowed to migrate toward FBS 10%. The total phase object area in the bottom (migrated cells) normalized to initial top value (seeded cells) was graphed over time. (*D*) Representative images of UCS1/2 cells in 3D organotypic cultures stained with phalloidin. (Scale bar: 50 μm.) (*E*) c-MycT58A is degradation-resistant and reverses antiproliferative phenotypes associated with Fbxw7 inactivation. The c-Myc antibody recognized both the wild-type and mutant forms.

and the T58A mutation renders the c-Myc protein insensitive to Gsk3β recognition and Fbxw7-mediated degradation (54). As already shown, endogenous c-Myc is degraded following Fbxw7 reexpression, while c-MycT58A proved resistant (Fig. 6*E*). c-MycT58A partially reversed the antiproliferative effect of Fbxw7 reexpression, demonstrating that c-Myc is one effector of the observed Fbxw7 phenotypes (Fig. 6*E*).

We then assessed the properties of 3D organoids derived from *Pten*, *Fbxw7*, or *Fbxw7*/*Pten* adult uteri not harboring overt tumors and grown in defined media (55, 56). *Pten* endometrial organoids were significantly larger than controls, but maintained spherical shape, a distinct epithelial monolayer, and hollow interior, giving them a characteristic "donut" morphology. *Fbxw7* organoids were also enlarged relative to *wt* controls, but exhibited a strikingly irregular and ruffled boundary of cells, a phenotype associated with loss of cell adhesion and propensity for invasion. Finally, *Fbxw7*/*Pten* organoids exhibited yet another distinct morphology, characterized by very large "cystic" organoids. Morphology and cell boundaries were more clearly delineated by cytokeratin immunofluorescence. *Fbxw7* organoids showed absence of a lumen consistent with an EMT phenotype, with loss of cell polarity demonstrated by the apical marker GM130. Cells in *Fbxw7*/*Pten* organoids demonstrated increased proliferation compared to their *wt* counterparts (*SI Appendix*, Fig. S7). These overall results are consistent with a role for *Pten* in driving cell proliferation and a synergistic role of *Fbxw7* in cell growth and in additional cellular phenotypes associated with EMT and invasive growth. This further rationalizes the observed potent cooperation among *Pten* and *Fbxw7* in tumor initiation and progression.

Evidence for a Role of Fbxw7 in the UCS Phenotype in Humans. *Fbxw7* mutations have been identified across several human EC histotypes, including endometrioid and serous adenocarcinomas, and also in UCS. These earlier findings suggested that *Fbxw7* mutations occur in UCS but did not ascribe a particular significance to them. To further explore this question, we analyzed available TCGA datasets for uterine adenocarcinomas (including endometrioid and serous subtypes) and UCS (6, 21). *Tp53* and *Fbxw7* mutations were much more likely to coexist in UCS vs. EC. Mutation incidences were compared for the genes most frequently mutated in UCS and plotted as the inverse of the *P* value of the difference between the 2 categories (EC vs. UCS, Fisher's exact test). Importantly, although several genes showed significant differences in mutation frequencies, among these, *Tp53* and *Fbxw7* were the only genes more frequently mutated in UCS (*SI Appendix*, Fig. S8 *A* and *B*). This supports our finding that *Tp53* and *Fbxw7* mutations synergize in the formation of UCS.

These findings raise the possibility that adenocarcinomas harboring *Fbxw7* mutations are more likely to develop into UCS. This is difficult to assess in humans because diagnosis of uterine cancer triggers hysterectomy, usually halting disease progression. However, to begin to explore this question, we studied a defined set of uterine adenocarcinomas subjected to next-generation sequencing of a comprehensive cancer gene panel (UNCseq) (57). We studied 28 cases harboring canonical *Fbxw7* mutations (WD40 hotspot or definite null mutations) and 20 cases without *Fbxw7* single nucleotide variants leading to amino acid alterations (*SI Appendix*, Table S3). All cases were subjected to IHC for L1CAM, a well-established marker for EMT in human ECs (58, 59). Notably, only Fbxw7-mutant tumors expressed L1CAM, and all of these were also p53-positive by IHC, although not all p53-positive cases harbored *Fbxw7* mutations (*SI Appendix*, Fig. S8 *C* and *D*). These results support the notion that Fbxw7-mutant adenocarcinomas have distinct properties and exhibit an EMT signature that distinguishes them from *Fbxw7*-wt adenocarcinomas.

Discussion

These studies implicate *Fbxw7* as a particularly important driver of UCS. While *Fbxw7* has been previously documented to undergo recurrent mutations in UCS, and could be surmised to be a tumor suppressor in UCS, prior studies had not pointed to *Fbxw7* as a specific driver of the unique clinicopathologic phenotypes associated with UCS (6, 21). Here, by taking advantage of defined genetic model systems, we showed that tumorigenesis driven by concurrent *Fbxw7* and *Pten* mutations progresses in a stereotypical manner. Neoplasia begins as well-defined EINs, which progress to well-differentiated endometrioid adenocarcinomas and then evolve into UCS with distinct epithelial and mesenchymal elements. This progression recapitulates many aspects of human endometrial carcinogenesis, including frequent squamous differentiation, heterologous differentiation, and aggressive clinical behavior with widespread metastasis upon progression to UCS.

This model provided a unique opportunity to identify cooperating oncogenic events. Specifically, although EINs were widespread, invasive carcinomas tended to arise focally (albeit with 100% incidence), as evidenced by the presence of invasive carcinoma in only one uterine horn. These observations strongly suggested that additional genetic event(s) were required for malignant progression. An unbiased approach based on resequencing of a comprehensive panel of known oncogenic drivers in human uterine cancer led to the discovery of *Trp53* as the singular and possibly obligate genetic mutation cooperating with *Fbxw7* and *Pten* in the genesis of UCS. However, one interesting observation was that *Trp53* mutations occurred as late events, since IHC showed that *Trp53* mutant clones arose within already invasive endometrioid adenocarcinomas. Thus, *Trp53* mutations did not appear to be specifically associated with invasion, but we cannot exclude the possibility that *Trp53* heterozygosity contributed to this transition. While *Trp53* and *Fbxw7* have distinctive if not unique roles as oncogenic drivers, mutations in a large number of PI3K pathway genes have similar biochemical consequences to *Pten* inactivation. For example, mutations in *Fgfr2*, *Kras*, *Pik3ca*, *Pik3r1*, or *Akt1/2/3* lead to constitutive activation of PI3K/Akt signaling, the central pathway misregulated in essentially all ECs. Our model suggests that the combination *Trp53* and *Fbxw7* mutations in the context of other alterations leading to PI3K pathway activation (through mutations in *Pten* or other factors) is strongly associated with the UCS phenotype. This study also provides further evidence that Fbxw7 is a strong p53-dependent tumor suppressor in UCS, as in other human cancers. For example, *Fbxw7* and *Trp53* strongly cooperate in murine models of colorectal cancer and T-cell lymphoma, and mutations frequently co-occur in human malignancies (60, 61). This genetic interaction is believed to be mediated by factors regulating cell cycle progression and cell growth, including Cyclin E, Notch, c-Jun, c-Myc, and mTOR, all of which are stabilized following *Fbxw7* mutation (53, 62). *Kras* appears to be another cooperating oncogene, as evidenced by one murine UCS harboring a mutation (present study) and the presence of *Kras* mutations in primary UCS (6).

EMT has been challenged as an organizing concept and terminology for the invasive and cell migration phenotypes that typify human carcinomas. For example, some have questioned experimental evidence interpreted as a switch of cell identity from epithelial to mesenchymal, such as vimentin expression. While UCS has stood as an exemplar for the occurrence of EMT in human cancer, such interpretations have also been challenged (63). Also, while more recent studies have shown that UCS components share a common clonal origin, questions have remained about the histogenesis and origins of the 2 elements in UCS; for example, if UCS represents an EMT or, conversely, MET (6). In this study, we conducted arguably the most rigorous demonstrations to date showing that UCS derives from epithelium. UCS arose in mice where Cre was induced only in epithelial cells, and where all of the invasive carcinomas arose from preexisting EIN that progressed to invasive adenocarcinomas. Finally, we conducted lineage tracing using the *mTmG* reporter (38), proving that the malignant mesenchymal components in UCS are descended from epithelium.

Using an addback system that permitted controlled reexpression of Fbxw7 in murine UCS lines, we demonstrated that Fbxw7 has an important and specific role as a driver of EMT—and one that is distinct from its cooperating drivers in UCS, Pten, and Trp53. In these experiments, we identified c-Myc, Notch-1, and Klf5 as likely Fbxw7 mediators of EMT. All 3 of these factors were significantly stabilized by Fbxw7 inactivation, and this stabilization was reversed by Fbxw7 reexpression. All 3 factors harbor Fbxw7 degron motifs and are well-known Fbxw7 substrates (13, 17, 53). While we cannot exclude the possibility that additional Fbxw7 substrates contribute to EMT in UCS, several observations suggest that these 3 factors are particularly important. Klf5 has been implicated in EMT, and, more recently, genetic alterations of the *Klf5* locus have been proven oncogenic, including focal amplification of *Klf5* superenhancers, as well as missense mutations in degron domains that disrupt Klf5–Fbxw7 interactions to stabilize Klf5 protein (49). The role of comparable *Klf5* mutations in EC has not been investigated, although *Klf5* is one of only 5 genes (with *Akt1* and *c-Myc*) implicated as EC heritable risk loci in GWAS studies (64). Klf5 protein is also stabilized in a conditional *Fbxw7* mouse model of intestinal cancer (19), underscoring that Klf5 is a general Fbxw7 target. c-Myc promotes cell migration, invasion, and metastases through multiple pathways, including the up-regulation of Snail, a transcriptional repressor that prevents the expression of E-Cadherin (65). Finally, Notch signaling promotes EMT and cell fate decisions during embryogenesis. Following receptor binding, a conformational change leads to cleavage and release of Notch intracellular domain (NICD), which translocates to the nucleus to modify gene expression of downstream targets such as *Snail*, *Hes*, *Hey*, and *c-Myc* (66). NICD contains a degron motif through which it is targeted by Fbxw7 for proteasomal degradation (67).

A remarkable aspect of this model is that 100% of tumors progressed into definitive UCS with heterologous differentiation. It is notable that, among a multitude of mouse models of EC, including many based on *Trp53*, *Pten*, or both, none have given rise to UCS, a finding that, in concert with our results, points to a specific role of *Fbxw7* as a driver of EMT and UCS (35, 36, 68). It is also notable that *Fbxw7*-based mouse models of other malignancies such as colorectal cancer have not developed carcinosarcomas (19), pointing now to this unique propensity of the endometrium (in both mice and humans). *Fbxw7*/*Pten* UCS arose from EIN, raising questions about the histological precursors of UCS in women. Although several pathways are possible, there is no well-described precursor lesion for UCS, either invasive

or preinvasive. There are no strict histologic criteria for UCS (2), but a single sarcoma focus >1 mm^2 is considered sufficient even in very large tumors (69), implying that progression from a preexisting adenocarcinoma is a regular occurrence. *Fbxw7* mutations are more frequent in UCS, but also occur in usual-type endometrioid adenocarcinomas, raising questions as to the natural progression of such tumors. Most uterine cancers are diagnosed relatively early due to vaginal bleeding and are effectively cured by hysterectomy. It is intriguing to speculate that *Fbxw7*-mutant endometrioid adenocarcinomas (were they left in the body) might have a propensity to progress into UCS, perhaps through the acquisition of *Tp53* mutations. This is further suggested by the fact that UCSs are more likely to harbor p53 mutations, and our finding that *Fbxw7*-mutant endometrioid adenocarcinomas are more likely to express L1CAM, a marker of EMT (59) frequently overexpressed in UCS (58). However, further investigations will be required to better define the natural history, precursors, and histologic intermediates for UCS.

Materials and Methods

A detailed description of mouse stocks and of allele and plasmid generation, antibodies used, cell line isolation, culture methods, tissue processing and staining, nucleic acid methods, Western blotting, and live cell imaging methods are provided in *SI Appendix, Materials and Methods*.

Animal Experimentation. All experiments were performed under a protocol approved by the University of Texas Southwestern (UTSW) Medical Center Institutional Animal Care and Use Committee.

Statistical Analysis. Error bars represent ±SEM; *P* values were calculated with GraphPad Prism V7.04 using the statistical tests described for each experiment unless otherwise indicated. For survival analysis, animals of the specified genotypes were assigned into aging cohorts at the beginning of the experiment and allowed to age undisturbed. Scoring of immunohistochemical staining intensity was performed by an investigator blinded as to the underlying genotype(s).

Data Availability. All data in this manuscript are freely available. The Sequence Read Archive (NCBI) accession number for the DNA sequencing data is SUV5613208. The GEO (NCBI) accession number for the RNA-seq data is GSE138490.

ACKNOWLEDGMENTS. This work was supported by Cancer Prevention Research Institute of Texas (CPRIT) Grant RP190207 and NIH/National Cancer Institute (NCI) Grants R01CA196912 and R01CA211339 to D.H.C. We acknowledge the assistance of the UTSW Medical Center Tissue Resource, a shared resource at the UTSW Medical Center Simmons Comprehensive Cancer Center, supported in part by NCI award number 5P30CA142543. The UTSW Medical Center Lyda Hill Department of Bioinformatics Core Facility, which provided infrastructure and data storage, was funded by CPRIT Grant RP150596. We gratefully acknowledge support from the UTSW Medical Center Transgenic Core Facility and Eduardo Bustamante (UTSW Medical Center Animal Resource Center).

1. R. L. Siegel, K. D. Miller, A. Jemal, Cancer statistics, 2019. *CA Cancer J. Clin.* **69**, 7–34 (2019).
2. R. J. Kurman, M. L. Carcangiu, R. H. Young, C. S. Herrington, *WHO Classification of Tumours of Female Reproductive Organs* (International Agency for Research on Cancer, Lyon, France, ed. 4, 2014), pp. 307.
3. L. A. Cantrell, S. V. Blank, L. R. Duska, Uterine carcinosarcoma: A review of the literature. *Gynecol. Oncol.* **137**, 581–588 (2015).
4. M. Saijo *et al*., Histologic appearance and immunohistochemistry of DNA mismatch repair protein and p53 in endometrial carcinosarcoma: Impact on prognosis and insights into tumorigenesis. *Am. J. Surg. Pathol.* **43**, 1493–1500 (2019).
5. X. Chen *et al*., Uterine carcinosarcomas: Clinical, histopathologic and immunohistochemical characteristics. *Int. J. Gynecol. Pathol.* **36**, 412–419 (2017).
6. A. D. Cherniack *et al*.; Cancer Genome Atlas Research Network, Integrated molecular characterization of uterine carcinosarcoma. *Cancer Cell* **31**, 411–423 (2017).
7. C. W. Ashley *et al*., Analysis of mutational signatures in primary and metastatic endometrial cancer reveals distinct patterns of DNA repair defects and shifts during tumor progression. *Gynecol. Oncol.* **152**, 11–19 (2019).
8. S. Jones *et al*., Genomic analyses of gynaecologic carcinosarcomas reveal frequent mutations in chromatin remodelling genes. *Nat. Commun.* **5**, 5006 (2014).
9. Y. Liu *et al*., Assessing inter-component heterogeneity of biphasic uterine carcinosarcomas. *Gynecol. Oncol.* **151**, 243–249 (2018).
10. E. C. A. Abeln *et al*., Molecular genetic evidence for the conversion hypothesis of the origin of malignant mixed müllerian tumours. *J. Pathol.* **183**, 424–431 (1997).
11. M. K. McConechy *et al*., In-depth molecular profiling of the biphasic components of uterine carcinosarcomas. *J. Pathol. Clin. Res.* **1**, 173–185 (2015).
12. S. Akhoondi *et al*., FBXW7/hCDC4 is a general tumor suppressor in human cancer. *Cancer Res.* **67**, 9006–9012 (2007).
13. N. Kourtis, A. Strikoudis, I. Aifantis, Emerging roles for the FBXW7 ubiquitin ligase in leukemia and beyond. *Curr. Opin. Cell Biol.* **37**, 28–34 (2015).
14. B. J. Thompson *et al*., Control of hematopoietic stem cell quiescence by the E3 ubiquitin ligase Fbw7. *J. Exp. Med.* **205**, 1395–1408 (2008).
15. W. Xu, L. Taranets, N. Popov, Regulating Fbw7 on the road to cancer. *Semin. Cancer Biol.* **36**, 62–70 (2016).
16. C. A. Cremona, R. Sancho, M. E. Diefenbacher, A. Behrens, Fbw7 and its counteracting forces in stem cells and cancer: Oncoproteins in the balance. *Semin. Cancer Biol.* **36**, 52–61 (2016).
17. C. H. Yeh, M. Bellon, C. Nicot, FBXW7: A critical tumor suppressor of human cancers. *Mol. Cancer* **17**, 115 (2018).
18. Y. Jiang *et al*., Fbxw7 haploinsufficiency loses its protection against DNA damage and accelerates MNU-induced gastric carcinogenesis. *Oncotarget* **8**, 33444–33456 (2017).
19. H. Davis, A. Lewis, A. Behrens, I. Tomlinson, Investigation of the atypical FBXW7 mutation spectrum in human tumours by conditional expression of a heterozygous propellor tip missense allele in the mouse intestines. *Gut* **63**, 792–799 (2014).
20. B. King *et al*., The ubiquitin ligase FBXW7 modulates leukemia-initiating cell activity by regulating MYC stability. *Cell* **153**, 1552–1566 (2013).
21. C. Kandoth *et al*.; Cancer Genome Atlas Research Network, Integrated genomic characterization of endometrial carcinoma. *Nature* **497**, 67–73 (2013). Erratum in: *Nature*. 500, 242 (2013).
22. C. M. Contreras *et al*., Lkb1 inactivation is sufficient to drive endometrial cancers that are aggressive yet highly responsive to mTOR inhibitor monotherapy. *Dis. Model. Mech.* **3**, 181–193 (2010).
23. E. A. Akbay *et al*., Cooperation between p53 and the telomere-protecting shelterin component Pot1a in endometrial carcinogenesis. *Oncogene* **32**, 2211–2219 (2013).
24. A. Guimarães-Young, T. Neff, A. J. Dupuy, M. J. Goodheart, Conditional deletion of Sox17 reveals complex effects on uterine adenogenesis and function. *Dev. Biol.* **414**, 219–227 (2016).
25. C. G. Peña *et al*., LKB1 loss promotes endometrial cancer progression via CCL2-dependent macrophage recruitment. *J. Clin. Invest.* **125**, 4063–4076 (2015).
26. K. Osoegawa *et al*., Bacterial artificial chromosome libraries for mouse sequencing and functional analysis. *Genome Res.* **10**, 116–128 (2000).
27. P. Soriano, Generalized lacZ expression with the ROSA26 Cre reporter strain. *Nat. Genet.* **21**, 70–71 (1999).
28. E. A. Jarboe, G. L. Mutter, Endometrial intraepithelial neoplasia. *Semin. Diagn. Pathol.* **27**, 215–225 (2010).
29. C. H. Spruck *et al*., hCDC4 gene mutations in endometrial cancer. *Cancer Res.* **62**, 4535–4539 (2002).
30. N. Eritja *et al*., Endometrial carcinoma: Specific targeted pathways. *Adv. Exp. Med. Biol.* **943**, 149–207 (2017).
31. J. Gao *et al*., Integrative analysis of complex cancer genomics and clinical profiles using the cBioPortal. *Sci. Signal.* **6**, pl1 (2013).
32. M. J. Goertz, Z. Wu, T. D. Gallardo, F. K. Hamra, D. H. Castrillon, Foxo1 is required in mouse spermatogonial stem cells for their maintenance and the initiation of spermatogenesis. *J. Clin. Invest.* **121**, 3456–3466 (2011).
33. E. D. Tarnawa, M. D. Baker, G. M. Aloisio, B. R. Carr, D. H. Castrillon, Gonadal expression of Foxo1, but not Foxo3, is conserved in diverse Mammalian species. *Biol. Reprod.* **88**, 103 (2013).
34. A. L. Strickland *et al*., PI3K pathway effectors pAKT and FOXO1 as novel markers of endometrioid intraepithelial neoplasia. *Int. J. Gynecol. Pathol.* **38**, 503–513 (2019).
35. A. M. Friel *et al*., Mouse models of uterine corpus tumors: Clinical significance and utility. *Front. Biosci. (Elite Ed.)* **2**, 882–905 (2010).
36. C. G. Peña, D. H. Castrillón, LKB1 as a tumor suppressor in uterine cancer: Mouse models and translational studies. *Adv. Exp. Med. Biol.* **943**, 211–241 (2017).
37. R. J. Zaino, R. J. Kurman, Squamous differentiation in carcinoma of the endometrium: A critical appraisal of adenoacanthoma and adenosquamous carcinoma. *Semin. Diagn. Pathol.* **5**, 154–171 (1988).
38. M. D. Muzumdar, B. Tasic, K. Miyamichi, L. Li, L. Luo, A global double-fluorescent Cre reporter mouse. *Genesis* **45**, 593–605 (2007).
39. A. Joshi, L. H. Ellenson, PI3K/PTEN/AKT genetic mouse models of endometrial carcinoma. *Adv. Exp. Med. Biol.* **943**, 261–273 (2017).
40. T. H. Kim, J. Y. Yoo, J. W. Jeong, Mig-6 mouse model of endometrial cancer. *Adv. Exp. Med. Biol.* **943**, 243–259 (2017).
41. X. Liang *et al*., The uterine epithelial loss of Pten is inefficient to induce endometrial cancer with intact stromal Pten. *PLoS Genet.* **14**, e1007630 (2018).
42. H. Zhang, FBXW7 is a defining driver of uterine carcinosarcoma by promoting epithelial-mesenchymal transition. BioProject. https://www.ncbi.nlm.nih.gov/bioproject/PRJNA543538. Deposited 17 May 2019.
43. D. Chakravarty *et al*., OncoKB: A precision oncology knowledge base. *JCO Precis. Oncol.*, 10.1200/PO.17.00011 (2017).
44. M. P. Kim, G. Lozano, Mutant p53 partners in crime. *Cell Death Differ.* **25**, 161–168 (2018).
45. G. Liu *et al*., High metastatic potential in mice inheriting a targeted p53 missense mutation. *Proc. Natl. Acad. Sci. U.S.A.* **97**, 4174–4179 (2000).
46. Y. Wang *et al*., Restoring expression of wild-type p53 suppresses tumor growth but does not cause tumor regression in mice with a p53 missense mutation. *J. Clin. Invest.* **121**, 893–904 (2011).

47. K. Yamato, M. Yamamoto, Y. Hirano, N. Tsuchida, A human temperature-sensitive p53 mutant p53Val-138: Modulation of the cell cycle, viability and expression of p53-responsive genes. *Oncogene* **11**, 1–6 (1995).
48. A. Yemelyanova *et al*., Immunohistochemical staining patterns of p53 can serve as a surrogate marker for TP53 mutations in ovarian carcinoma: An immunohistochemical and nucleotide sequencing analysis. *Mod. Pathol.* **24**, 1248–1253 (2011).
49. X. Zhang *et al*., Somatic superenhancer duplications and hotspot mutations lead to oncogenic activation of the KLF5 transcription factor. *Cancer Discov.* **8**, 108–125 (2018).
50. D. Zhao, H. Q. Zheng, Z. Zhou, C. Chen, The Fbw7 tumor suppressor targets KLF5 for ubiquitin-mediated degradation and suppresses breast cell proliferation. *Cancer Res.* **70**, 4728–4738 (2010).
51. V. Close *et al*., *FBXW7* mutations reduce binding of NOTCH1, leading to cleaved NOTCH1 accumulation and target gene activation in CLL. *Blood* **133**, 830–839 (2019).
52. I. C. Cuevas, D. H. Castrillon, FBXW7 is a defining driver of uterine carcinosarcoma by promoting epithelial-mesenchymal transition. Gene Expression Omnibus (GEO). https://www.ncbi.nlm.nih.gov/geo/query/acc.cgi?acc=GSE138490. Deposited 7 October 2019.
53. B. L. Sailo *et al*., FBXW7 in cancer: What has been unraveled thus far? *Cancers (Basel)* **11**, E246 (2019).
54. S. R. Hann, Role of post-translational modifications in regulating c-Myc proteolysis, transcriptional activity and biological function. *Semin. Cancer Biol.* **16**, 288–302 (2006).
55. M. Y. Turco *et al*., Long-term, hormone-responsive organoid cultures of human endometrium in a chemically defined medium. *Nat. Cell Biol.* **19**, 568–577 (2017).
56. M. Boretto *et al*., Development of organoids from mouse and human endometrium showing endometrial epithelium physiology and long-term expandability. *Development* **144**, 1775–1786 (2017).
57. N. M. Patel *et al*., Improved tumor purity metrics in next-generation sequencing for clinical practice: The integrated interpretation of neoplastic cellularity and sequencing results (IINCaSe) approach. *Appl. Immunohistochem. Mol. Morphol.*, 10.1097/PAI.0000000000000684 (2018).
58. M. Versluis *et al*., L1CAM expression in uterine carcinosarcoma is limited to the epithelial component and may be involved in epithelial-mesenchymal transition. *Virchows Arch.* **473**, 591–598 (2018).
59. J. Chen, F. Gao, N. Liu, L1CAM promotes epithelial to mesenchymal transition and formation of cancer initiating cells in human endometrial cancer. *Exp. Ther. Med.* **15**, 2792–2797 (2018).
60. I. Onoyama *et al*., Conditional inactivation of Fbxw7 impairs cell-cycle exit during T cell differentiation and results in lymphomatogenesis. *J. Exp. Med.* **204**, 2875–2888 (2007).
61. K. Y. Jen *et al*., Sequential mutations in Notch1, Fbxw7, and Tp53 in radiation-induced mouse thymic lymphomas. *Blood* **119**, 805–809 (2012).
62. J. Perez-Losada, J. H. Mao, A. Balmain, Control of genomic instability and epithelial tumor development by the p53-Fbxw7/Cdc4 pathway. *Cancer Res.* **65**, 6488–6492 (2005).
63. D. Tarin, E. W. Thompson, D. F. Newgreen, The fallacy of epithelial mesenchymal transition in neoplasia. *Cancer Res.* **65**, 5996–6000 (2005).
64. T. H. Cheng *et al*.; National Study of Endometrial Cancer Genetics Group (NSECG); Australian National Endometrial Cancer Study Group (ANECS); RENDOCAS; AOCS Group, Five endometrial cancer risk loci identified through genome-wide association analysis. *Nat. Genet.* **48**, 667–674 (2016).
65. N. Venkateswaran, M. Conacci-Sorrell, MYC leads the way. *Small GTPases*, 1–9 (2017).
66. K. M. Capaccione, S. R. Pine, The Notch signaling pathway as a mediator of tumor survival. *Carcinogenesis* **34**, 1420–1430 (2013).
67. M. R. Broadus *et al*., Identification of a paralog-specific Notch1 intracellular domain degron. *Cell Reports* **15**, 1920–1929 (2016).
68. T. Daikoku *et al*., Conditional loss of uterine Pten unfailingly and rapidly induces endometrial cancer in mice. *Cancer Res.* **68**, 5619–5627 (2008).
69. R. Murali *et al*., High-grade endometrial carcinomas: Morphologic and immunohistochemical features, diagnostic challenges and recommendations. *Int. J. Gynecol. Pathol.* **38** (suppl. 1), S40–S63 (2019).